

Master Thesis

Effect of vortex shaking on the resistivity of
type-II superconductors



By

Stefan J. Menzi

Physics Institute
of the
University of Zurich

Supervised by
Prof. A. Schilling

August 29, 2007

Contents

1	Introduction	1
2	The Theory	2
2.1	Superconductivity	2
2.1.1	High-Temperature Superconductors	2
2.1.2	The melting transition	5
2.2	Vortex shaking	6
2.3	Sample	7
3	The Experiment	11
3.1	Design	11
3.2	Electrical contacts	12
3.3	Testphase	12
3.4	Measurements	14
3.5	A New Material...	19
3.6	...and a new shaking technique	20
4	Interpretation and Conclusion	27
4.1	$NdBa_2Cu_3O_{7-d}$	27
4.2	$LuNi_2B_2C$	28
5	Appendix	29

1 Introduction

The decision to write a master thesis about superconductivity was founded on two different motivations. The first was my general interest in this amazing phenomenon, which is as well theoretically as practically of great importance and very promising for the future. My second motivation was that it gave me the possibility to conduct a whole experiment from its planning to its conclusion, step by step, and offered a diverse range of work, from the designing of the setup to the assembling of the experiment and in the end to its interpretation.

The main goal of this master thesis was to find out if the characteristics of the resistivity at the liquid-to-solid phase transition of a clean single crystal in a magnetic field can also be seen in a slightly disordered crystal, which is addressed by using a process called vortex shaking, the application of an ac magnetic field perpendicular to the main field to the crystal, which should “shake” vortices trapped in pinning centers into their equilibrium state. Vortex shaking is a relatively new technique, thereby opening a lot of new possibilities for interesting discoveries.

This work was conducted under the supervision of Prof. Dr. Andreas Schilling and with the help of his research group at the University of Zurich.

2 The Theory

2.1 Superconductivity

Superconductivity is today, as it has been for many years now, a very active field in modern solid-state physics research and although that many scientists are dedicated to it, there are still a lot of unanswered questions. Areas like Low T_c Superconductivity (LTS) are now thought to be fully understood, but especially High T_c Superconductivity (HTS) is still full of open questions, as the Bardeen-Cooper-Schrieffer-Theory (BCS)[1], which works so fine for LTS does not hold anymore for HTS. But as many experiments during the last decades have shown, the supercurrent in high-temperature superconductors is still carried by these pairs of correlated electrons. It is now the goal of superconductivity research to find a consistent theory to explain this strong mechanism that keeps the Cooper pairs together, and hence to explain how HTS really works. This understanding could lead to an even further raise of the transition temperatures for the onset of superconductivity like some authors, e. g. Ashcroft[2], believe even up to room temperature. The work that we have been doing should help to gather some more insights, so that eventually all the pieces of the puzzle can be put together and reveal the whole picture of high-temperature superconductivity.

As I already treated the phenomenon of superconductivity in general in my Bachelor Thesis, I will not discuss the general topic here further. For more information about superconductivity I refer to literature such as “Supraleitung” of W. Buckel[4] and my Bachelor Thesis[5].

2.1.1 High-Temperature Superconductors

The first high-temperature superconductor was found by Karl A. Müller and Johannes Bednorz in 1986[6], a discovery which was immediately recognized by the Nobel Prize in Physics in 1987. The LaBaCuO compound they studied had a critical temperature of 30K, which was very much unexpected, as this cuprate-perovskite material was a ceramic and as such almost an insulator at room temperature. Later on more and more cuprates with even higher critical temperatures were discovered, really earning their name as soon as they crossed the critical temperature of liquid nitrogen at 77K, making it far easier and especially cheaper to handle superconductors. All high-temperature superconductors are type-II superconductors, which means that they only show a partial Meissner effect above a certain lower critical magnetic field B_{c1} . Beyond B_{c1} , in the so-called mixed state, the magnetic field penetrates the material in flux lines (vortices), which form a so-called Abrikosov lattice

for lower temperatures and a vortex glass or fluid for higher temperatures without destroying the cooper pairs. The circular currents forming the flux lines and mark a border between normal and superconducting regions.

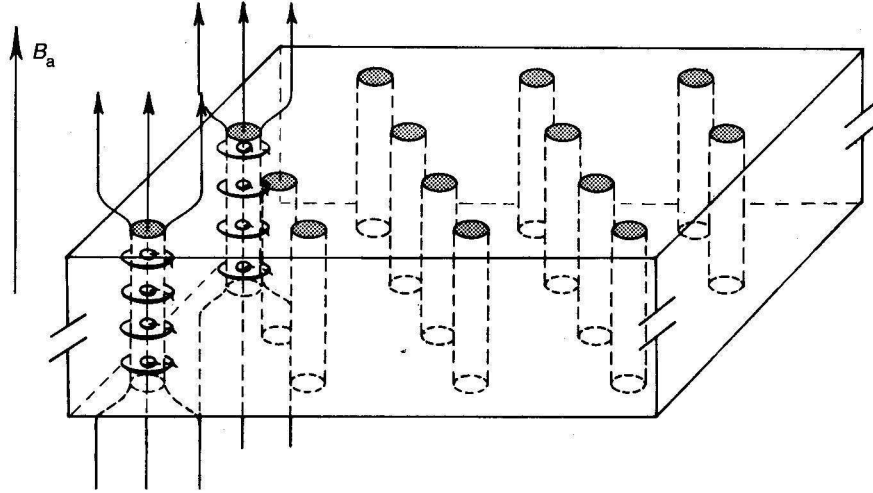


Figure 1: Shubnikov-Phase (“mixed state”) in a Type II superconductor with the Abrikosov lattice.

The mixed state, in which magnetic flux flows through the material, is called the Shubnikov¹ phase. Under the right conditions (low temperatures, small currents and a field strength below $B_m(T)$, the melting line), the vortices form a rigid lattice, called Abrikosov² lattice, named after Abrikosov who first predicted it[7]. If a current is flowing through the superconductor in this mixed state, it produces a Lorentz force acting on the vortices. In an ideal superconductor without any defects this force would generate a motion of the vortices, hence a motion of the lattice. Real superconductors however have all some sorts of defects or impurities, like grain boundaries, dislocation walls, voids, etc., where the magnetic flux gets trapped and which act as “pinning centers” for the vortices, keeping them and with them the whole

¹Lev Vasilyevich Shubnikov, 1901 - 1937, Russian physicist and experimenter

²Alexei Alexeyevich Abrikosov, born 1928 in Moscow, co-recipient of the 2003 Nobel Prize in Physics

lattice in place. But as soon as any of the afore mentioned conditions rise above certain, material dependent values, the vortex lattice begins to move or even melt. The individual vortices start to move, first just a wobbling at their place, then through the material, when the pinning forces and the lattice are no longer strong enough to hold them against the Lorentz force. The movement is perpendicular to the current and the field[8]. This possibility for the vortex lattice to melt at sufficiently high temperatures, makes the phase diagram and the behavior of a HTS significantly different from other low T_c type-II superconductors, see figure 2 and [11], as the melting transition marks the onset of a finite resistivity well inside the superconducting regime, see figures 20 and 21 in the appendix.

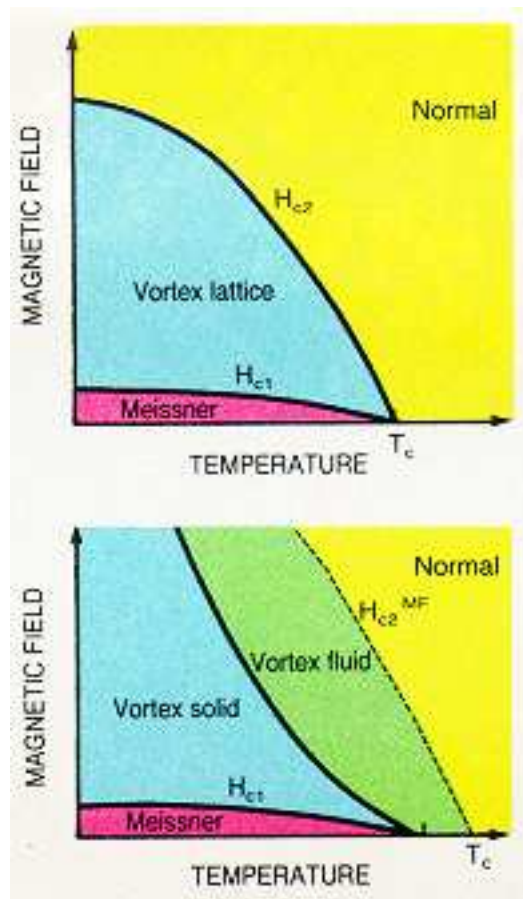


Figure 2: Phase diagrams of a conventional low temperature and a high T_c type-II superconductor.

2.1.2 The melting transition

Let us have a closer look at the melting of the vortex lattice. In order to do this, we must first gather some more insights into the main characteristics of high-temperature superconductors. All the HTS's are based on copper oxides, compounds made out of electrically conducting CuO_2 layers and insulating layers of other oxides. This layered structure leads to an extreme anisotropy with an anisotropy parameter $\gamma \gg 1$. The anisotropy parameter γ stands for the relation between perpendicular and parallel magnetic penetration depth. Another extreme property of high-temperature superconductors is the dimensionless Ginzburg-Landau parameter $\kappa = \lambda/\xi$, the relation between the magnetic penetration depth λ and the coherence length ξ , the minimal length for a change in the superconducting order parameter Ψ . In a HTS type-II superconductor, λ is unusually large, whereas ξ is extremely small, resulting in a $\kappa \gg 1$. E. g. BSCCO (Bi2223) has a κ of over 130, lead on the other hand, a low-temperature superconductor with a T_c of 7.2K, has a κ of 0.47. (This gives one of the criteria for the definition of the difference between type-I and type-II superconductors, given by Abrikosov: If κ is smaller than $1/\sqrt{2} \simeq 0.71$ the superconductor is of type-I, if it is bigger than $1/\sqrt{2}$ then it is a type-II.) Now, the elastic properties of the vortex lattice depend heavily on these parameters. The smaller ξ and the larger λ is, the softer are the vortices and the weaker the stabilizing forces on them, meaning that they are easier to move out of their lattice positions. For an anisotropic superconductor these movements are even a factor γ stronger than for an isotropic one. All these factors lead to very "bendable" vortices under marginal mechanical stress, which are, because of the relatively high temperatures, subject to strong thermal fluctuations. For low enough temperatures, the vortices are bound to natural pinning centers and form a regular Abrikosov lattice, but as soon as the temperature reaches a certain value T_m , which might be far below T_c in strong magnetic fields, the thermal fluctuations get strong enough to rip the vortices out of their positions. This results in the melting of the lattice, just like ice melts. The melting follows approximately the so-called Lindemann-criterion, which states that the melting occurs when the thermal fluctuations of the vortices reach a certain fraction (5 to 20%) of the mean distance between vortices in the lattice, see [9],[10]. Once the melting took place, the vortices are able to move freely through the material, unbound from any pinning centers. In this phase, vortices can be seen as interacting, particle like objects, resembling cooked spaghetti[11]. If a current is applied to the superconductor the motion of the vortices due to the Lorentz force leads to the development of a longitudinal potential gradient in the superconductor, which accounts for an energy loss in

the fluid, observed as a finite resistance in the still superconducting regime. This energy loss happens due to several mechanisms: The most important one is the motion of the normal-conducting core inside the vortices through the material, where its electrons are scattered on the thermal lattice vibrations, resulting in Joule losses. Another source of energy loss is the so-called thermal mechanism of dissipation. Vortex motion is always accompanied by energy absorption in the region of the forward boundary of the vortices where the superconducting phase changes into the normal phase. This leads to the appearance of microscopic thermal gradients accompanied by heat flow and energy dissipation[17]. Furthermore the vortices lose energy on encountering pinning centers, etc. This is why it can happen that the resistance of a high-temperature superconductor doesn't immediately drop to zero when T_c is reached. It rather stays finite, although falling significantly faster than before T_c , until the melting line is reached. There the vortices stop moving and settle in their lattice position and the resistivity finally drops to zero, but only if the material is very clean and has very few pinning centers. Otherwise the ever less mobile vortices get trapped in a pinning center and the equilibrium lattice can't properly form and critical currents keep circulating in the material. This leads again to a delay of the onset of zero resistivity, which holds on for a few Kelvin until the binding forces of the lattice get strong enough to bring the trapped vortices into equilibrium.

2.2 Vortex shaking

Since the early 1970s it is known that a small oscillating ac magnetic field applied perpendicular to the main field B influences the depinning current density and can strongly modify the transport properties of type-II superconductors in the flux-flow state [12]. Later in the 1990s it was observed by Willemin *et al.*[13], that the application of such an ac field leads to a fast depinning of the vortex lattice and hence to significant growth of the reversible domain in the magnetic field (H) versus Temperature (T) plane of a high-temperature superconductor. The theoretical basis for this effect was established by E. H. Brandt *et al.* in [14] and was later on advanced by G. Mikitik and Brandt in a series of papers, see [15] and citations therein. Vortex shaking is, generally speaking, a process to literally shake vortices out of their pinning centers into their equilibrium state. This leads to a relaxation of the vortex lattice and therewith to the mentioned growth of the reversible domain in the (H,T) phase diagram of a high-temperature superconductor, which is needed e. g. to study various typical parameters within the so-called London model, which needs a thermodynamic equilibrium of the mixed state [13], [18]. In this experiment we try to apply this technique to see directly

on one single crystal the difference in resistivity between a melting transition where vortices are held in pinning centers and one where they are in equilibrium.

The technique works as follows: Consider a thin superconducting strip that fills the space $|x| \leq w, |y| < \infty, |z| \leq d/2$ with $d \ll w$, and a constant homogeneous external magnetic field H_a which is directed along z , while an ac magnetic field $h_{ac} = h \cos \omega t$ is applied along x , perpendicular to H_a and to the shielding currents in the sample. We make the Bean assumption that the critical current density j_c does not depend on the local induction B [19]. The currents flowing in the critical state of the strip generate a nonuniform distribution of the magnetic induction $B_z(x)$, as the self-field of the currents adds to h_{ac} on the upper (or lower) plane of the strip and reduces it on the opposite plane. As a result, the applied ac field periodically tilts the vortices in this state. However, at each point x with a nonzero sheet current $J(x)$ (the current density integrated over the thickness d), the tilt is not symmetric relative to the central plane of the strip $z = 0$, and during each cycle of the ac field, the asymmetry leads to a drift of vortices towards the center $x = 0$ of the strip. This shift tends to equilibrate $B_z(x)$, and it also generates a dc electric field which decreases $J(x)$. When $J(x)$ reaches zero, the asymmetry disappears, and the process stops [16].

Unfortunately, the above treatment is only valid for currents flowing perpendicular to the ac field. As it is very unlikely to have an almost infinitely long and thin superconducting sample for the experiments, it is necessary to treat longitudinal shaking, with currents flowing parallel to the ac field as well. This is somewhat more complicated. We have now again the same setting as above, but this time h_{ac} is parallel to the sheet current J which flows in y direction. The vortices are again tilted by the ac field, this time from z towards the y direction. This happens because the critical-current density $j_c(z) = [j_{cx}(z), j_{cy}(z), 0]$ has a nonzero x component which is antisymmetric in z , $j_{cx}(z) = -j_{cx}(-z)$. Thus, $j_c(z) = j_c(z)[- \sin \phi(z), \cos \phi(z), 0]$ flows at an angle $\phi(z)$ to the y axis. Since the Lorentz force applied to an infinitesimal element of the vortex is normal to $j_c(z)$, and the element drifts along this force, the tilt along y is always accompanied by a small drift along x . This drift is independent of the sign of h_{ac} , and hence, under the influence of an ac field, the vortex will drift in the direction of $[J_y \times H_z]$ by an oscillating screwlike motion. The mechanisms are further explained in Figures 3 and 4.

2.3 Sample

The sample used for this first experiments was a $NdBa_2Cu_3O_{7-d}$ crystal, optimally doped and twinned. Its critical temperature was ≈ 96.7 K. Nd-

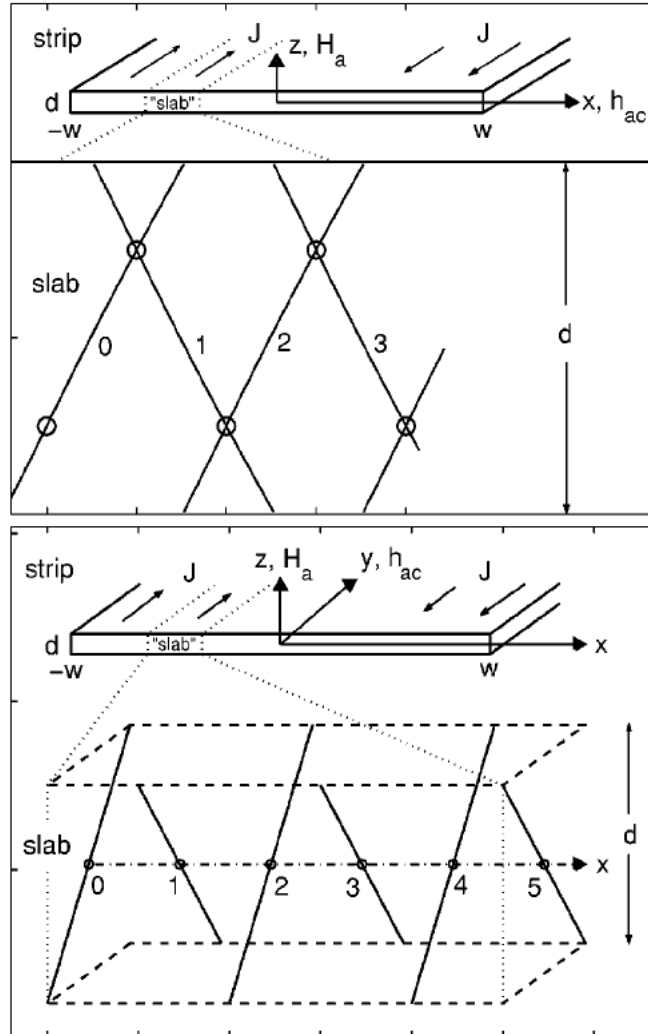


Figure 3: Visualization of the transverse and longitudinal vortex shaking. In both geometries the vortices drift towards the center of the strip. Shown is one vortex at subsequent times $t\omega/\pi = 0, 1, 2, \dots$. Top: If h_{ac} is transverse to J , the vortices “walk” in the xz plane (the vortices are straight since here $J_c \ll h_{ac}$, H_a is assumed). Bottom: If h_{ac} is parallel to J , the vortices periodically tilt in the yz plane and at the same time move along x . From [15].

BaCuO has basically the same structure as YBCO and is therefore a layered and anisotropic, thus typical, representative of the famous copper oxides (see figure 5). The temperatures at which the melting transition occurs are

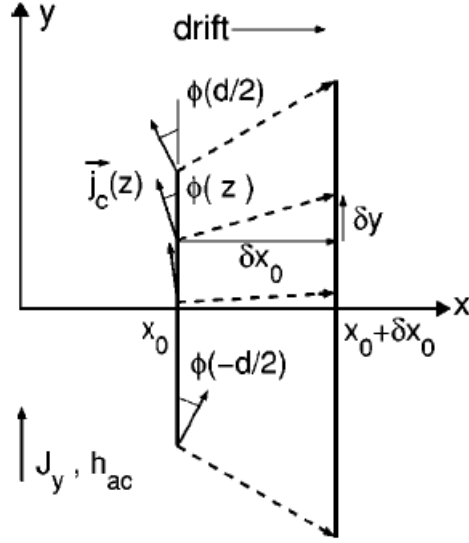


Figure 4: Scheme of the vortex shift in a slab when the longitudinal ac magnetic field is increased from h_{ac} to $h_{ac} + \delta h$. Shown is the projection on the xy plane of a vortex (bold solid line) which tilts more away from the z axis and at the same time shifts from $x = x_0$ to $x = x_0 + \delta x_0$. The projected shifts of some vortex line elements are shown as dashed arrows with components δx_0 and $\delta y(z)$, $\delta y(z) = -\delta y(-z)$. These arrows are along the Lorentz force, which is perpendicular to the local current density $j_c(z)$ (solid arrows) lying in the xy planes at the angle $\phi(z)$ to the y axis. From [15].

plotted for different magnetic fields in figure 6.

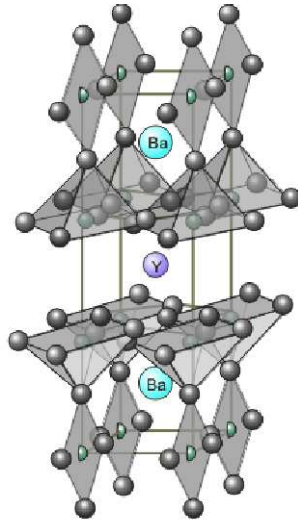


Figure 5: Structure of YBCO with the CuO_2 planes. In NdBCO the Yttrium atoms are replaced by Neodymium.

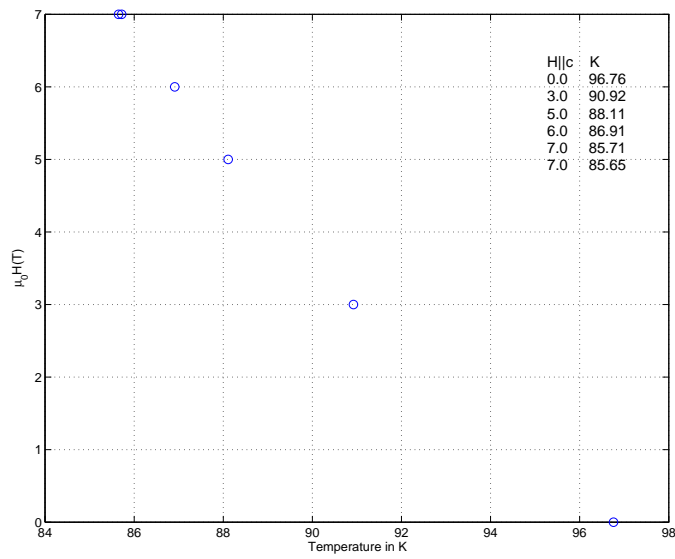


Figure 6: Location of the melting transition in the magnetic phase diagram. (Data from specific-heat measurements.)

3 The Experiment

3.1 Design

The experimental setup was as follows: As a base plate I used a synthetic sapphire disk, which was chosen because of its good thermal conductance and electrical insulation. On top of it, on the right, a copper 'gibbet' was attached with GE-Varnish to the sapphire to support the crystal. On the left side, a copper coil for the ac field was set on an unattached copper plate, making it possible to move it over the crystal and back again. This coil had an inductance of about 0.20 mH, with about 200 windings producing a magnetic field of $\sim 1.8 - 3$ Oe/mA. See sketch 7 and sketch 22 in the appendix for further details of the setup.

Unfortunately it took an immense amount of time to gather and prepare these components due to the variety of people and institutions involved and the Christmas holiday break, which delayed the delivery of the sapphire platelets for almost a month.

Originally a four-wire resistivity measurement was planned, but due to the problems mentioned in 3.3, only two-wire measurements could be made.

The system used to measure the resistivity and to drive the coil was the

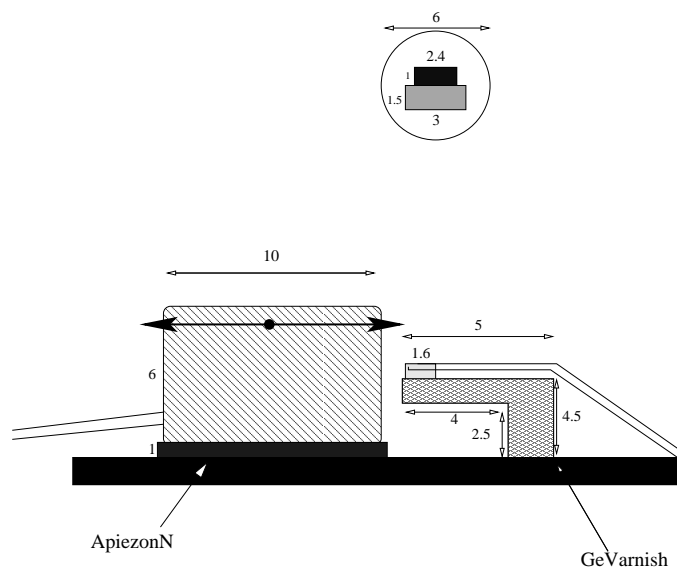


Figure 7: Sketch of the experimental setup, side view.

Physical Property Measurement System (PPMS) of Quantum Design, see [3] and [5], with the optional AC Transport Option.

3.2 Electrical contacts

The first task was to connect the sample to the already existing PPMS Resistivity Puck on which it was mounted together with the rest of the setup. Because of the small dimensions of the crystal and malfunctioning silver epoxy this proved to be rather difficult. My first attempts failed utterly and when even with better silver epoxy and refined manual techniques no significant progress could be achieved, we figured that probably the surface of our crystal itself might be the problem. Oxygen atoms of the surface could have left its topmost layers, thus creating an insulating layer on the surface and raising the contact resistance unfavorably. In order to solve this problem, the crystal was baked in an oven under an oxygen atmosphere at 460°C for seven consecutive days, but again, the attempt to get a good contact to the crystal (i.e. a contact resistance of about $1\ \Omega$), could not be achieved. The next step was then to “rejuvenate” the surface, and the crystal was put in a 1% Bromine-Methanol solution for half an hour which was supposed to roughen the surface, thus making it more accessible to the anew oxygen treatment in the oven, this time at 430°C for one day, with the conducting silver epoxy contacts already applied. This treatment proved to be successful. The new contacts had a resistance of about $1\ \Omega$, as desired.

3.3 Testphase

To test the contacts and the proper working of the PPMS, the resistivity of the crystal was first measured in zero field. The results showed that something was still wrong, because already above the critical temperature the resistance went considerably *below* zero Ohm, below T_c the resistance was higher as before and after some oscillations even rising with decreasing temperature, thus being completely unphysical. Further tests revealed that these results were reproducible, and that the oscillations right below T_c smoothed out in an applied magnetic field.

Doubts about the calibration of the PPMS and the intactness of the used puck, the measuring platform on which the sample assembly was mounted, could be excluded by measuring a piece of iron as reference sample, which produced good results.

The only other probable explanation for the “negative” resistance was that the currents in the crystal, as cuprate superconductor, of course layered, took some other, wound paths than the expected straight one. To sort that possibility out, I conducted a two-wire resistivity measurement on the crystal by removing the voltage contacts from the crystal and short-circuiting the voltage and current contacts of the puck. This did actually solve the

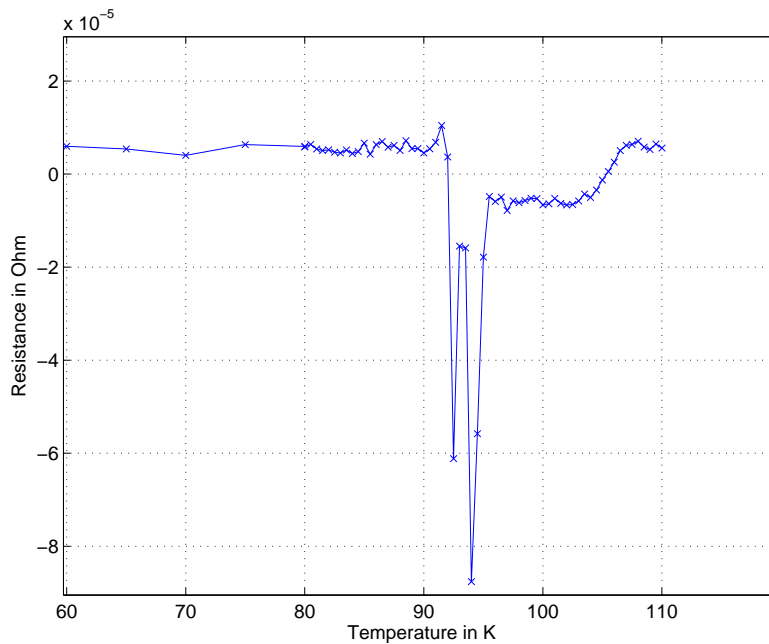


Figure 8: Example of the first unsuccessful measurements at 0 Tesla, where the resistance becomes “negative”. T_c is at 96K.

problem and reasonable results were obtained, that now included the additional resistance of the underground of the measuring setup (wires, contacts, ...), however this led us to believe that just the two voltage contacts on the crystal might have been the problem, so I remade them, this time using a different wiring than the one proposed in the manual. This resulted in a constantly positive resistance, but below T_c the resistance was still too high and rising with falling temperature. Confronted with this (until now unexplained) oddities we decided to do our measurements with the two-wire method, though with lower precision, but without this significantly unphysical behavior. Later, the coil producing the ac shaking field was attached to the remaining free current contacts of the puck and finally first tests with vortex shaking could be made.

These did not at all meet our expectations, this time with a rather obvious reason, I discovered that we had seriously underestimated the Lorentz forces on a coil under ac current in a 9T magnetic field. The coil was completely detached from its copper support, far away from the crystal and in a ninety degree angle to it. Obviously no shaking could have taken place in that manner. To prevent this from happening again, the coil was placed into a big

droplet of GE-Varnish, which was then dried in an oven at 50°C for better stability. Later, the free copper support platform of the coil was also attached to the sapphire disk, as the vibrations induced by the ac field caused the contacts from the coil to the puck to break. These measures were at least partially successful as the setup was now stable until fields of 9T main and ≈ 5 Oe ac magnetic field. Of course, the solution of this problem was instantly followed by the next one. The following measurements were conducted with the parameters (x/y/z) where x stands for x mA measuring/coil current, y for y Hz measuring/shaking frequency and z for z seconds measuring/shaking time either for the resistivity measurements or the shaking coil. As mentioned above, 1mA of current in the coil induced a magnetic field of $\sim 1.8 - 3$ Oe. The first measurement with the new attachment for the coil was conducted at (2/1000/0.1) for shaking, (1/79/1) for measuring and at 9T main field, and the coil attachments were stable. The results, however, showed a lot of unsystematic scatter in the data (see figure 9), which could not be explained and which were present also in subsequent measurements with the same parameters. Interestingly this problem could be solved by just changing the shaking parameters. I took the parameters that were used by Willemin *et al.* in their 1998 paper [13]: (8/581/8).

Now that all the initial problems seemed to be solved, the main experiment could be started.

3.4 Measurements

To start with, I measured the resistance of the NdBCO crystal in a range from 100K to 75K, for main fields of 0, 1, 3, 5, 7 and 9T with parameters of (1/79/1) measuring and (8/581/8) shaking, resulting in a ac field of ~ 18 Oe. As a reference, the resistance curves for every field strength were first measured without the activation of the ac field. In the beginning, the temperature was set to a 100K, far above the critical temperature of 96K for NdBCO, then the field was changed and then the resistance was measured every 0.25K, each temperature three times down to 75K. The measurements *with* shaking field were started in the same way, again every 0.25K data points were taken, now the first one before a shaking took place, then one immediately after the shaking and a third one after a 4s relaxation time. The results of the run without shaking looked promising, pretty much as expected. Because of the two-wire measurement the background of the wires and contacts was of course still visible and there was a slight field dependent offset. After the subtraction of these unwanted parts the critical temperature and the field dependency of the transition were nicely visible in the graph (see figure 10). The results for the run with shaking however, were, to our

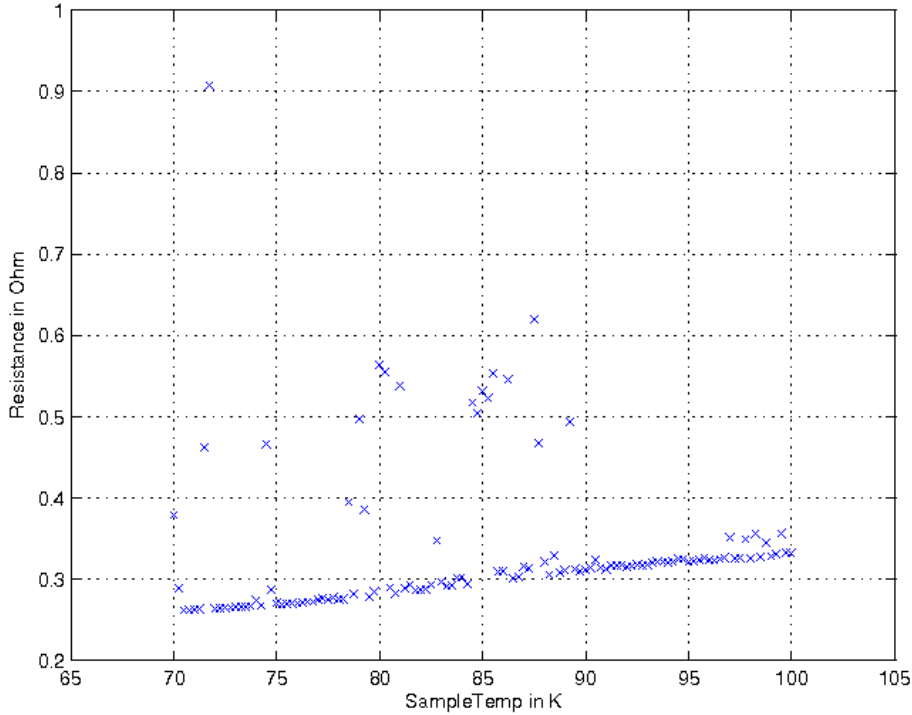


Figure 9: Scattered data in the graph of the 9T (2/1000/0.1) measurement.

disappointment, almost exactly the same as the ones where no shaking took place. A slight difference could be seen, so obviously something did happen during the shaking, but the difference was not nearly as big as we expected and not even reproducible or only at the expected places. Figure 11 shows in the upper left corner the curves for the resistivity of NdBCO at 7T both with active and inactive coil, which are too identical to be distinguishable from each other. The background is not subtracted yet. On the upper right, an enlargement of the region where the melting is expected to take place is shown, crosses representing the measurements of the first run without shaking, the stars represent in chronological order the measurement before the shaking, the one immediately after the shaking and one 4s after the shaking. As can be seen, there is no significant difference between the respective results. The third part of figure 11 on the bottom shows the difference between the curve without and the curve with shaking, which should theoretically be zero at the beginning and go sharply to $\approx 0.01\Omega$ around 85K, then again decrease to zero Ω around 80K. Obviously this is not the case. The curve oscillates always just around zero and there is no difference below and above

the supposed melting point. All these findings are valid for all other main fields too. Every measurement was repeated several times, with altered contacts, different wirings of the crystal and the coil and even on different machines, but the results were always the same: no difference between data taken with or without shaking could be found.

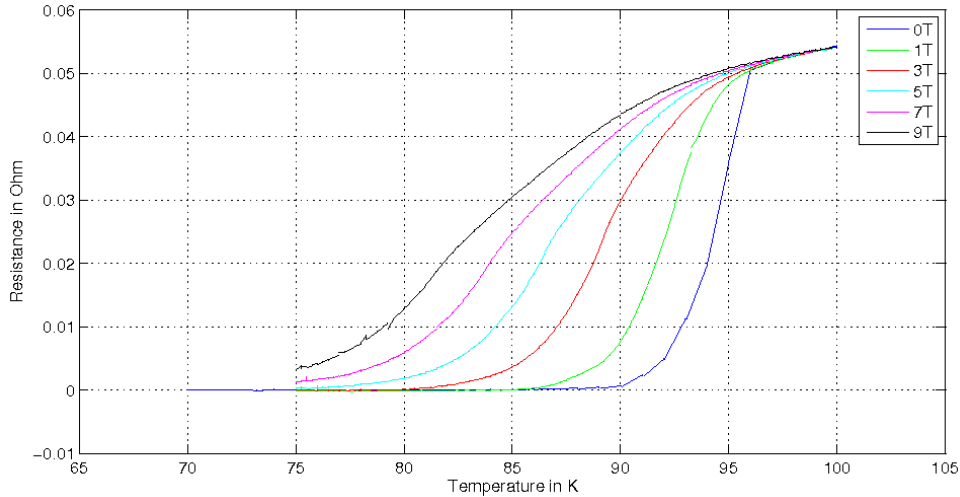


Figure 10: Results for the measurements of the resistance of NdBCO without shaking. Background and offset distracted.

One of the circumstances suspected to be the reason for this were the parameters of the shaking, which could lead to a too weak or even too strong shaking. So several tests with different shaking parameters were executed next. For the main field I chose a smaller magnetic field (5T) as before, to avoid tearing the coil loose again and the temperature was set to 100, 90 and 85K with a full set of measurements for each temperature. At first the amplitude of the coil current was changed, currents of 2, 4, 8, 12 and 16mA were tested, corresponding to ac-field strengths of 4 to 36Oe, then several different frequencies were measured (59, 231, 367, 457, 581, 787, 997Hz) and finally the shaking time was altered (1, 2, 4, 6, 8, 10s). None of these diverse parameters lead to a different result than the one already known. The only insight gained, was that the resistance of the NdBCO crystal depended quite heavily on the frequency used, but as later similar measurements proved, there was no general rule to describe that properly. The first time it was measured, the resistance got slightly lower with higher frequencies, the second time, after some weeks and hence not with exactly the same setup, the resistance grew quite heavily, almost quadratic, with

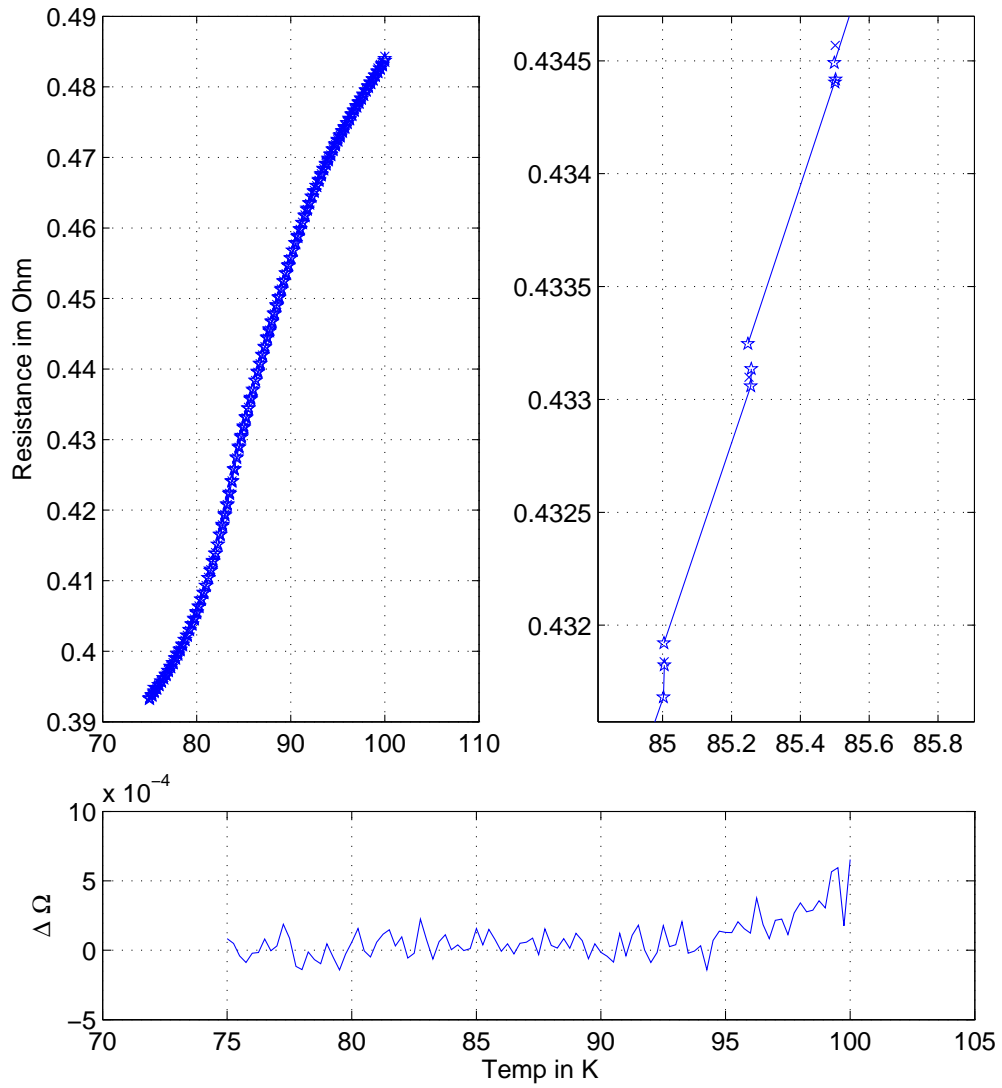


Figure 11: Results for the measurements at 7T with and without shaking. Upper right: Zoom into the region of the melting transition. Crosses representing the run without shaking, stars the run with shaking. Bottom: Difference between the normal and the resistance with shaking.

higher frequencies. Probably these dependencies came not only from the

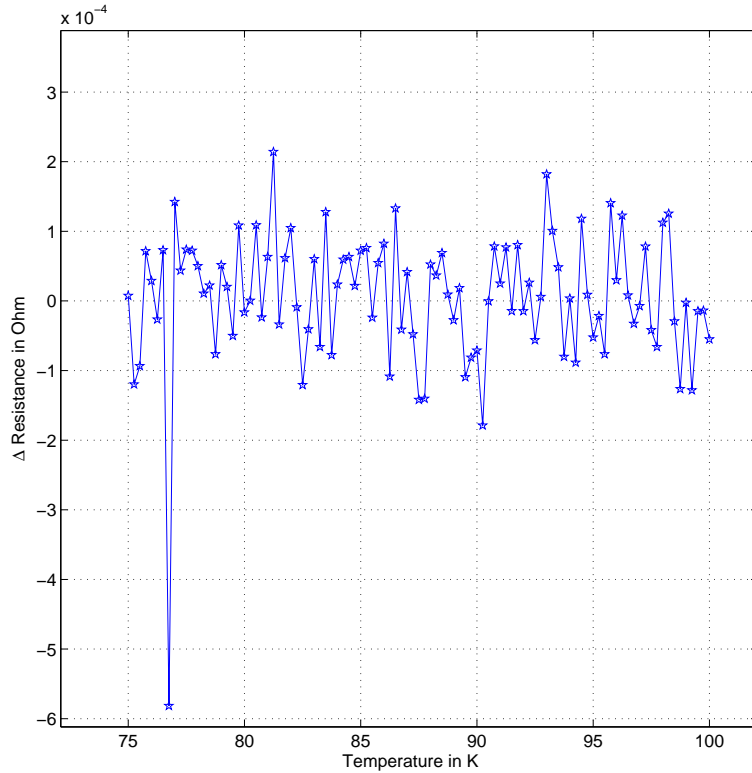


Figure 12: This figure shows the difference between measurements with and without shaking for 9T main field. Obviously, the shaking did not have an observable effect.

crystal itself, but also from effects the frequency had on the coil and on the measurement method.

Up to this stage of our investigations, every measurement was taken *after* a certain shaking period, because the PPMS could not measure two samples at the same time, which was theoretically not a disadvantage, but at that time this was regarded as a probable reason for the null-results. So the setup of the experiment was changed to allow a simultaneous shaking and measuring. This was done by placing the coil in series to the measuring current circuit. Naturally this design did not allow measurements without shaking anymore and so further on only one set of parameters is needed as the shaking and measuring currents are now the same. The first measurements of this type were again conducted with (8/581/8) and at 5T. In this setup the system had

some problems in finding an appropriate gain and had to switch it several times during one run, leading to unstable measuring results. As a few tests revealed, this could be fixed by just changing the parameters to (8/231/8), proving the frequency dependence of the resistance again. The gain was stable until roughly 300Hz and then became more and more unstable. Now that we did not have a reference measurement for the sample in the natural disequilibrium state we needed to know what we were looking for in our measured curves. We would expect a relatively sharp drop of the resistance in the last third of the non-zero resistance part of the superconducting phase, just below the melting transition, in contrast to a smooth curve. But again, no feature of this kind could be seen, although the same set of measurements as with the previous measurements had been performed.

3.5 A New Material...

As it became obvious that the remaining time would not be sufficient to plan and conduct a totally new setup to solve our problem with NdBCO, which would have involved a time consuming modification of the chronically fully booked PPMS, we decided to try a similar task with a quite different material: $LuNi_2B_2C$, being an intermetallic compound (instead of a cuprate) of the form Ln-Tr-B-C, where Ln is a lanthanide element (Y, Ho - Lu) and Tr a transition metal (Pd or Ni). It is a type-II superconductor with a transition temperature of $\approx 16.6K$. This compound is not layered as the copper oxides are, but instead shows a 3D-structure, as shown in figure 13.

In $LuNi_2B_2C$, we were looking for a possible feature in the resistance just below T_c , where peaks have been seen in measurements of the specific heat by M. Reibelt, a Ph.D. Student of our group.

The first tests were done with a two-wire measurement, just to find the right orientation of the crystal with respect to the field, and the coil was again placed in series with the measuring current circuit. To my surprise these measurements showed again resistance values that were negative, this time even with the two-wire method, and had a strange temperature dependence. To check these results I switched from the AC Option to the Resistivity Option of the PPMS and repeated the measurements. Now the resistance values came out positive, but the temperature dependence was still not as it should be. Instead of a general decrease with falling temperature, the resistance was growing heavily down to T_c , then dropped sharply for a while, and began then to rise again. At higher magnetic fields the transition could not even be found until 3K. But this time we had several pieces of the same crystal at our disposal, so I took another one with a different surface and surface orientation and made it ready for a four-wire measurement, to make

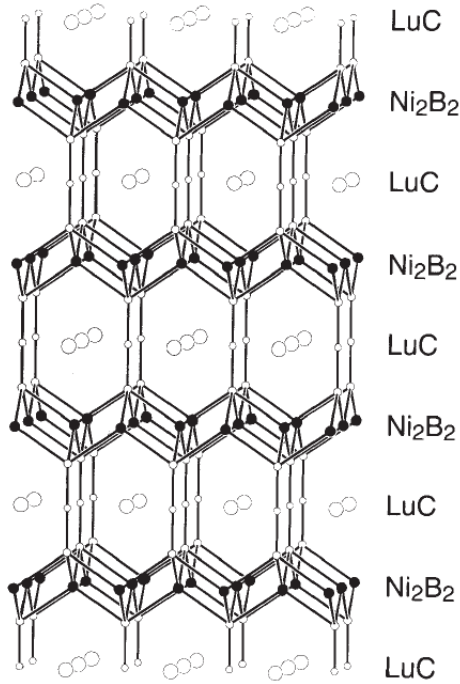


Figure 13: The crystal structure of $\text{LuNi}_2\text{B}_2\text{C}$. Filled circles are Ni atoms, the largest open circles are Lu atoms. The Ni-B-C framework is indicated by the bonds between the atoms. [26]

sure that the crystal was not the source of the problem. The contact resistance was good from the beginning, $\approx 2\Omega$, and no further preparation of the crystal was needed as it was the case with the NdBCO crystal. But also this second piece with a completely new four-wire connection and a separate connection for the coil displayed the same results, as shown in figure 14 and 15. And again, shaking did not make any serious difference.

3.6 ...and a new shaking technique

The last series of tests that we made after we started with the $\text{LuNi}_2\text{B}_2\text{C}$ crystal involved a new shaking technique, which was already used by M. Reibelt for his experiments on the LuNiBC crystals. To bring the vortices into their equilibrium state, he used a method first mentioned by G. Ravikumar *et al.* [27]. They did not use an ac magnetic field perpendicular to the main field to shake the vortices, but instead they applied a number of small cycling loops of the main field prior to a measurement to the crystal. To

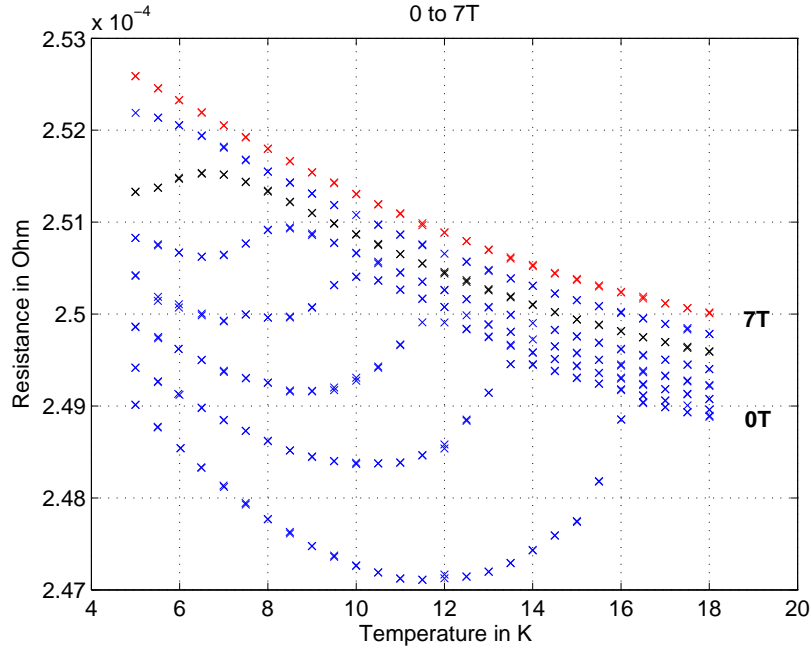


Figure 14: Temperature vs Resistance of the LuNiBC crystal from 0 to 7T, with shaking.

explain this effect we once again need Bean's critical state model [19], but this time it needs to be altered so that J_c becomes a history dependent J'_c , in order to be compatible with experimental facts. The details are explained in the paper of G. Ravikumari *et al.* [27], where they come to the conclusion that $J'_c = J_c + (|\Delta B|/B_r)(J_c^{st} - J_c)$, where the parameters J_c^{st} (stable current density) and B_r (retardation parameter) are only assumed to be uniquely determined by B and T. The consequences of this new J'_c are, that it allows J_c to depend on the magnetic history of the system, thereby lifting the restriction on the uniqueness of J_c imposed in the Bean model and that J_c can be different from J_c^{st} but that such a state is metastable. The metastable J_c is driven to its stable value J_c^{st} by a change in the local field B, independent of its sign, as ensured by the absolute value $|\Delta B|$ in J'_c . This evolution of J_c is shown schematically in section (i) of figure 16, when the initial J_c is both larger and smaller than J_c^{st} and for both increasing and decreasing B from the ambient value in each case. Additionally, section (ii) of figure 16 shows a similar approach to J_c^{st} , when the field is cycled. Physically, we may imagine that in the absence of thermal fluctuations it is the change in local field B that can move the vortices from their metastable configuration into

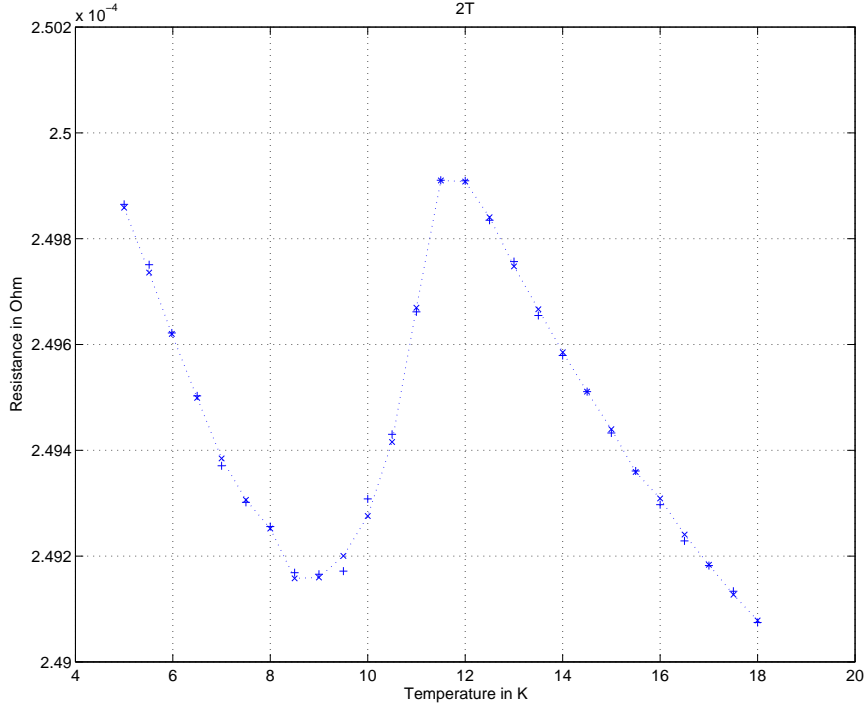


Figure 15: Temperature vs Resistance of the LuNiBC crystal at 2T, with shaking. \times represent pre-shaking results, $+$ results after shaking. The dotted line follows the \times as an aid.

the stable one [27]. So much for the theory.

The setup was the same as before (four-wire measurement, but no coil) and the experiment was then conducted as follows: From the measurements of M. Reibelt it was known that the peak only showed after some dozens of field cycles or if the sample was cooled down very fast (-200mK/s), if the sample was slowly cooled (-0.2mK/s) and no cycles were made, the peak has not been visible. So the first run was one with slow cooling and no field cycles. The sample was first cooled to 18K, then a field of $\mu_0 H = 2.5T$ was applied. The further cooling was made with a dT/dt of -0.2mK/s down to 4.3K. The resistivity was then measured from 4.3 to 11K in small steps. When this was done, the sample was again heated to 18K to bring it back into its initial state. The next run was again slow cooling and involved 60 cycles of the main magnetic field with a $\mu_0 \Delta H = 0.1T$ (i.e. from 2.5 to 2.6T and back again). Runs number 3 and 4 were both with fast cooling (-200mK/s),

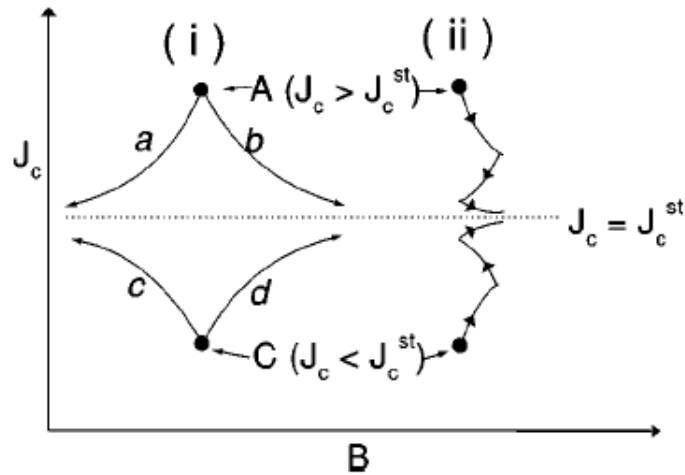


Figure 16: To approach of the current density J_c towards J_c^{st} is schematically shown as a function of field B for a fixed J_c^{st} . (i) At point A, $J_c > J_c^{st}$ and J_c decreases when the field is increased (path b) or decreased (path a). Similarly, at point C, $J_c < J_c^{st}$ and J_c increases when the field is increased (path d) or decreased (path c). (ii) The same is shown under the application of an oscillatory field. [27]

number 3 without cycles, run 4 with 60 cycles. The results, as expected, still showed the strange temperature dependence the sample had exhibited in earlier measurements, but these runs involving a cycling of the field did actually show a clearly visible feature in resistivity which the runs without cycling did not show. Figure 17 shows the results for the two slow cooling measurements, where the feature can be seen at $\approx 9.8K$. In the next figures, figures 18 and 19 and figures 23 and 24 in the appendix, the additional, approximately quadratic, rise in resistance has been subtracted for better clarity. It can easily be seen in figure 24 that in our case the velocity of the cooling did not have an effect, as it had in the specific heat measurements. Figure 19 shows an enlargement of the area around the peak in the cycling runs, showing that the feature is pretty good reproducible. This was the last measurement done and concluded the experimental phase of the work.

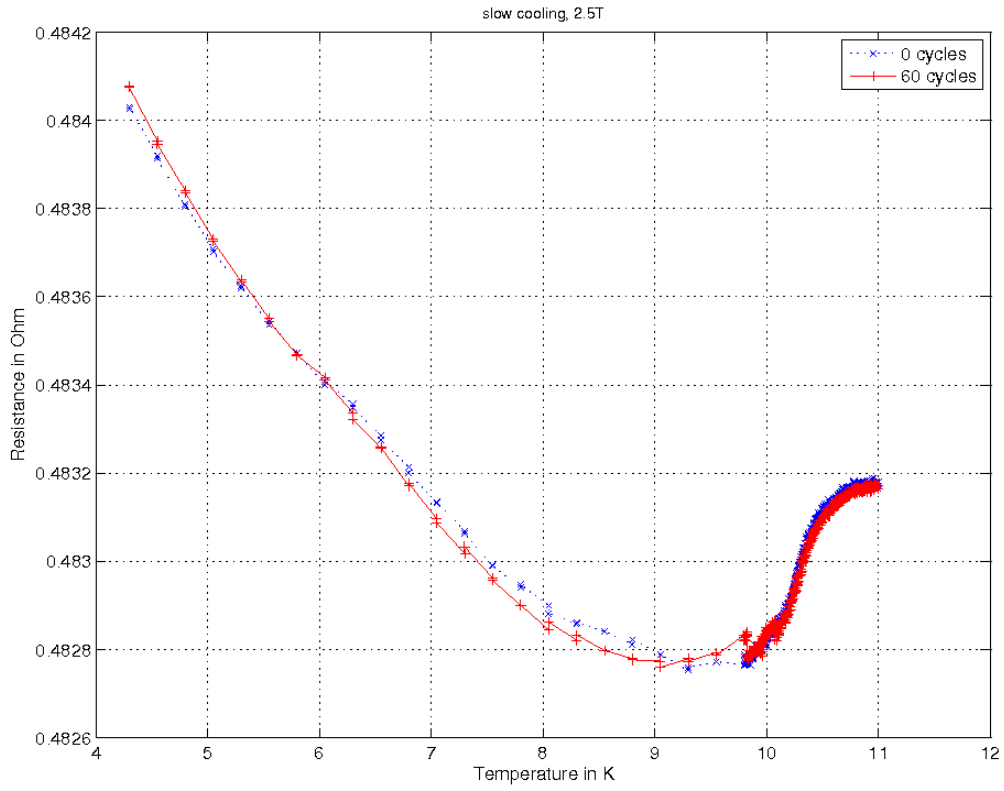


Figure 17: Results for the two slow cooling measurements, the feature can be seen at $\approx 9.8K$.

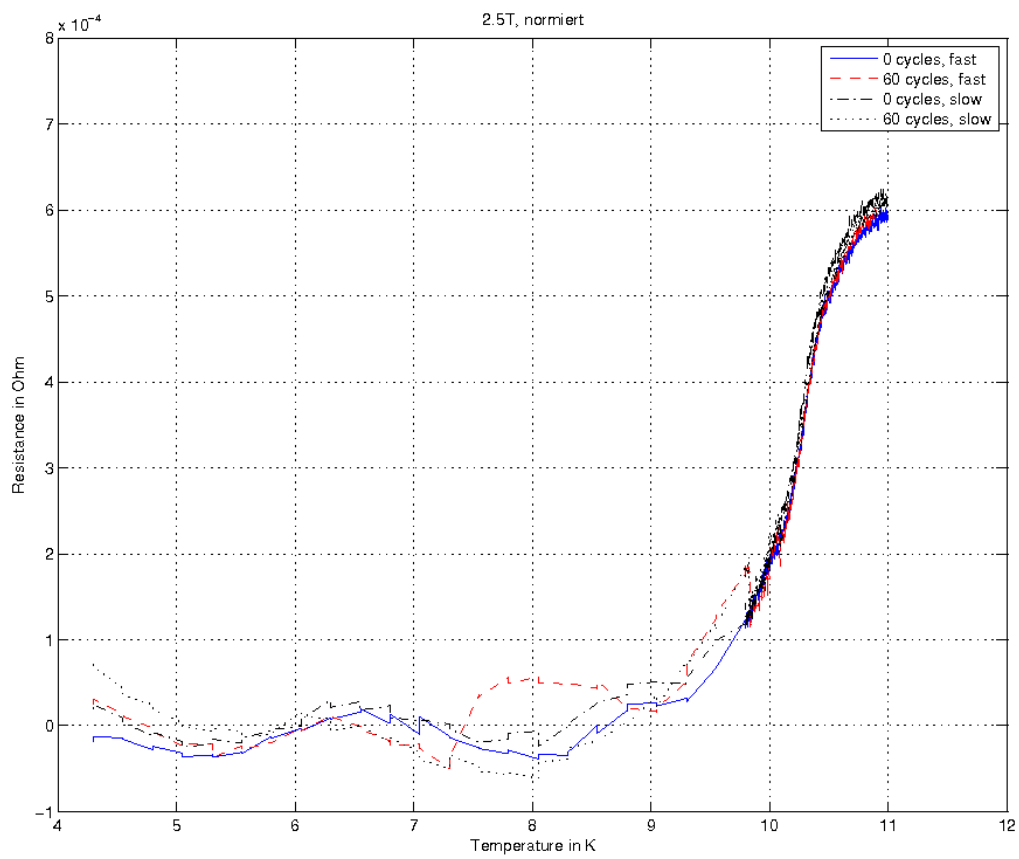


Figure 18: Results of the second LuNiBC experiments. Adjusted data for all four runs.

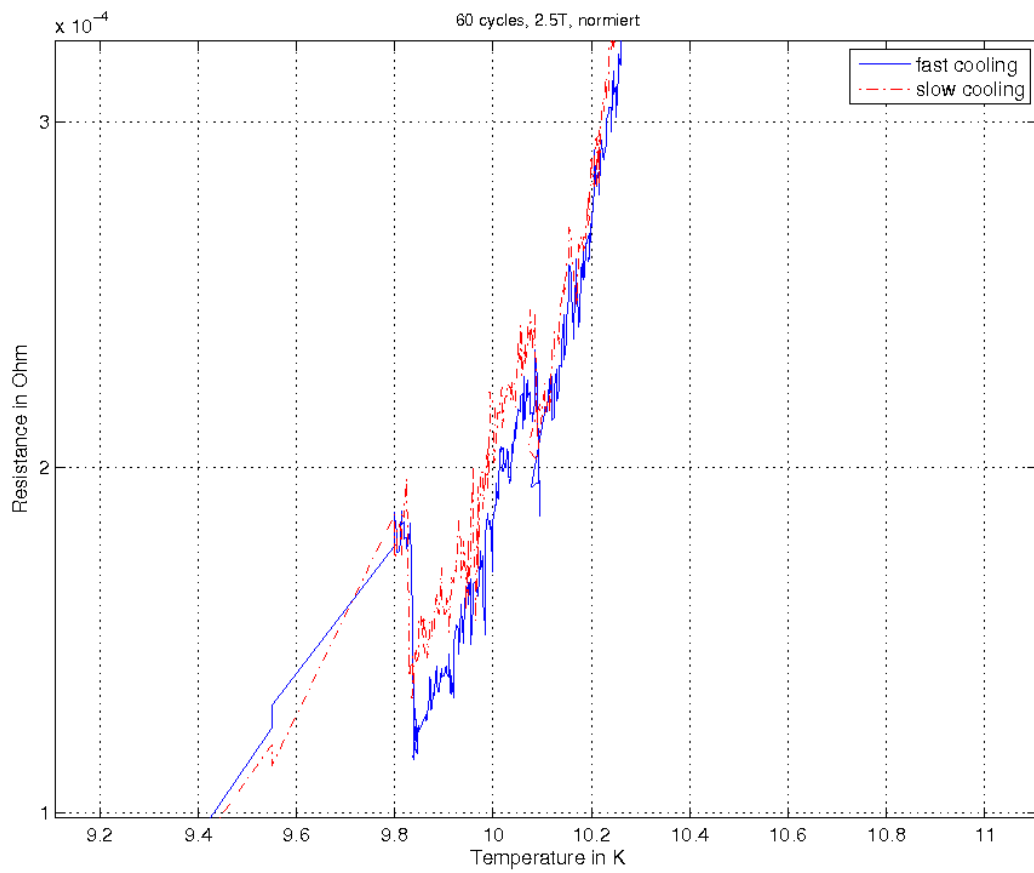


Figure 19: Zoom into the area around the feature. Within the experimental scatter, the two features (after fast and slow cooling) are nearly identical.

4 Interpretation and Conclusion

4.1 $NdBa_2Cu_3O_{7-d}$

As discussed earlier, no melting transition could be found in NdBCO, i.e. we could not distinguish between measurements with or without shaking. Of course, this can be due to many very different reasons. The most obvious would be that the shaking itself did not work, due to a malfunctioning coil or inadequate shaking parameters. But as far as I can say, the coil was working fine. There was definitely an ac current flowing in it, as the strong Lorentz force it experienced and the resistivity measurements that were done automatically on the coil have proved. There is no reason why the coil should not have induced a magnetic field and indeed a tiny difference between each of the separate runs could actually be seen, as mentioned in the first part of 3.4, but of course it was not nearly of the magnitude we expected. This brings us to the shaking parameters. Within the limits of our technical possibilities I tried every reasonable combination of applied current (i.e. field strength), frequency and shaking time (i.e. number of vortex “steps”), but not one of them was successful. Additionally one can add that the used parameters had already been proved to be working by Willemin *et al.* in their experiments. I conclude that the shaking was working properly and the reason that no difference in resistance showed up has to be elsewhere. A. K. Pradhan *et al.* report in their 1999 paper [28] that they encountered a strong dependence of the transition on the oxygen partial pressure during the growth of the crystal. They measured “a smeared first-order melting transition (FOT) for 0.01 and a distinct FOT for 0.03% and 0.05%, and a continuous transition for 0.07% [O_2 partial pressure to Ar atmosphere during growth]”. It is not known to me in what percentage of O_2 our crystal was grown. Additionally, as mentioned in sub-chapter 3.2, we treated it with a 1% Bromine-Methanol solution and had it in an oven under oxygen atmosphere to improve its surface, so it is quite possible that the crystals surface was under conditions similar to the crystals of Pradhan with 0.07% O_2 partial pressure, which means that the transition of our crystal was not distinct as expected, but instead actually genuinely continuous and the vortex shaking could not have had an effect. As the magnitude of disorder of both crystals, the NdBCO and the LuNiBC, was as well not known, it is also possible, that the pinning forces in the crystals were too strong for any kind of vortex shaking, as vortex shaking is normally only used in just slightly disordered crystals, where the vortices are not far away from equilibrium. The most fundamental question is at last, if vortex shaking influences resistivity measurements at all, this question arises because of the fact, that resistivity measurements need a current, which does naturally not

result a real equilibrium. The measuring currents might in fact destroy the effects of the shaking immediately. In order to prove this thesis, resistivity experiments should be made with crystals where the melting transition has already been found with magnetization measurements or similar methods, where the measurement itself does not destroy the equilibrium.

4.2 $LuNi_2B_2C$

In the beginning, the $LuNi_2B_2C$ measurements showed the same unsatisfactory results as NdBCO, *plus* a peculiar temperature dependence seen in figure 14. For the effects of shaking the same arguments as before are again applicable, but the unexpected temperature dependence is even more difficult to explain. Later measurements (not described here) with the same setup, but again on the second PPMS, did no longer show the “S” shaped curves that are caused by the onset of superconductivity and the quadratic slope as in the first measurements, the superconducting transition could not even be found any more. This leads me to believe that the crystal, or at least its surface, must have become non-superconducting, most probably because of the silver epoxy contacts, which also may have caused the increase of the resistivity with falling temperature.

Now to the second part of the $LuNi_2B_2C$ experiment. Naturally it is the topmost question why this feature arises and especially why it is an upward and not a downward peak as our vortex shaking theory proposes. A second question arises from the comparison with the data from M. Reibelt. His peak in the specific heat for 2.5T is at $\approx 10.5K$ while the peak seen here is at 9.8K. This might just be due to different thermometer calibrations, but a comparison of ΔT , the difference between T_c and the peak position, shows that his peak is quite closer to T_c as our feature, $\Delta T_{(c_p)} \approx 0 - 0.4K$, where $\Delta T_{(\Omega)} \approx 1.2K$. So we might in fact have found another effect that is responsible for our feature. Let us return to the first question, which could be the answer to this question as well. The fact that the feature is an *increase* in resistance instead of a drop and at a considerably lower temperature as the suspected melting transition is probably an indication that the sample was still not in equilibrium state. But a well-founded explanation for this effect can not be given without more experiments and more theoretical knowledge. It can only be stated here, that the magnetic history of the sample had in fact a considerable effect on the measured resistivity, which supports the findings of M. Reibelt.

I’d like to thank Prof. Schilling for the possibility to do this thesis and his supervision, and his group and other members of the institute for their kind help.

5 Appendix

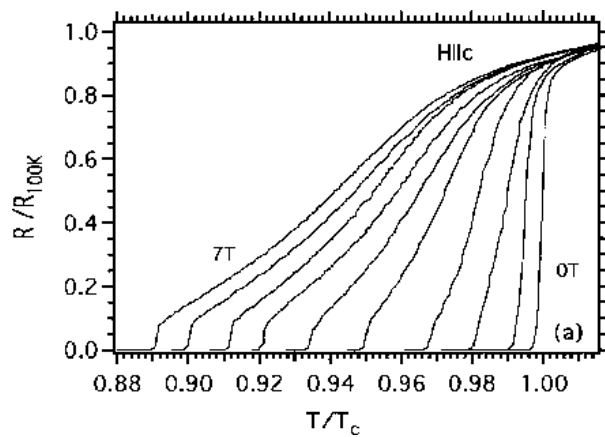


Figure 20: In-plane resistance $\rho(H, T)$ of a clean high-temperature superconductor. After [28].

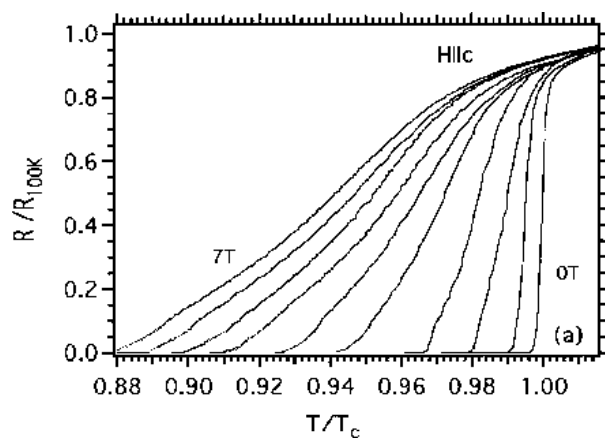


Figure 21: In-plane resistance $\rho(H, T)$ of a high-temperature superconductor with pinning centers, without shaking.

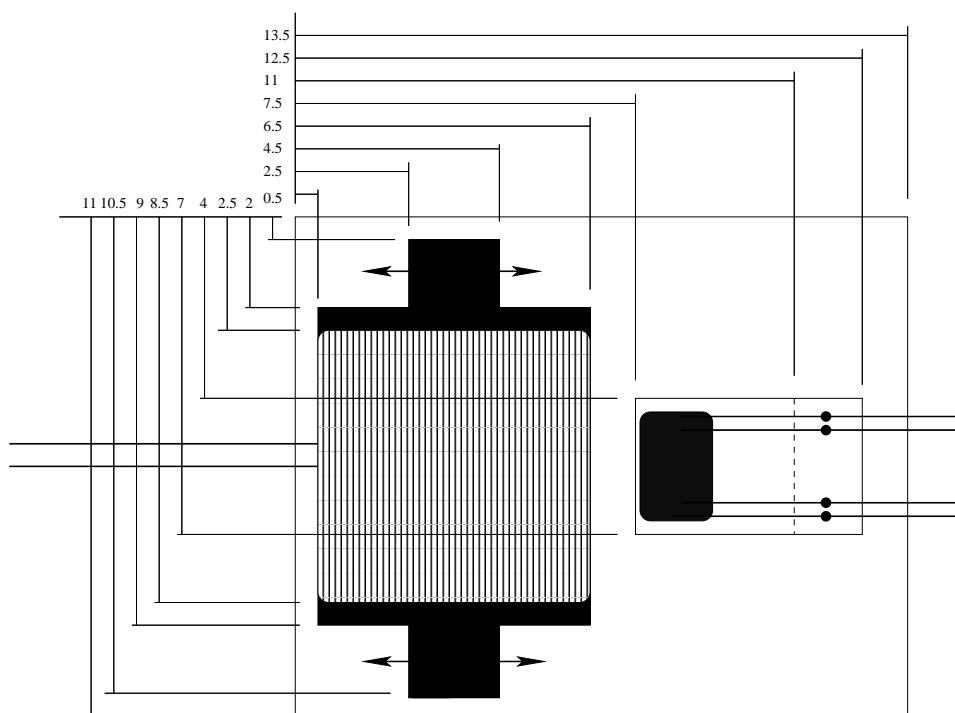


Figure 22: Sketch of the experimental setup, top view.

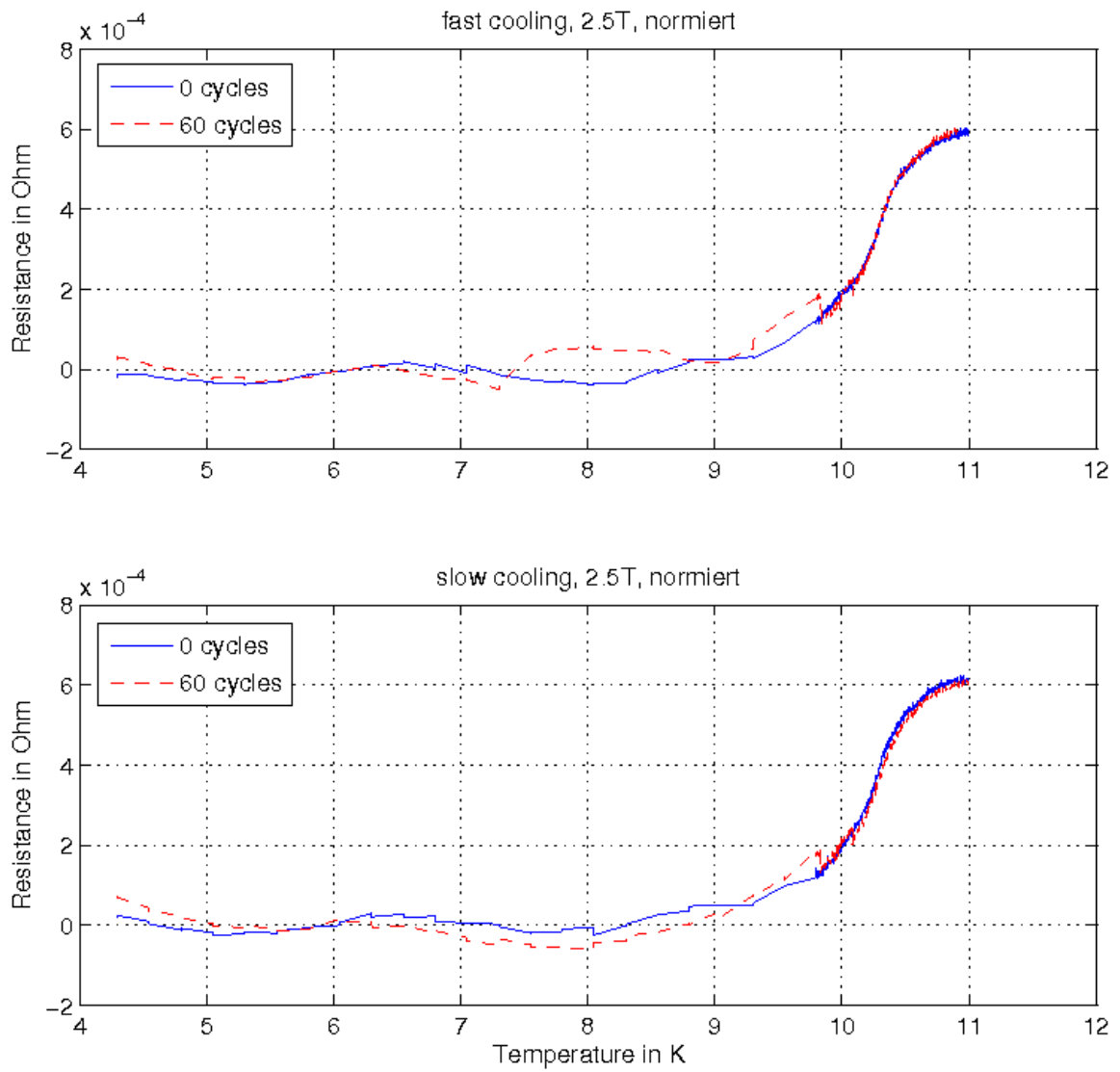


Figure 23: Comparison of fast and slow cooling in the second $LuNi_2B_2C$ experiment. The feature at 9.8K is both times clearly visible.

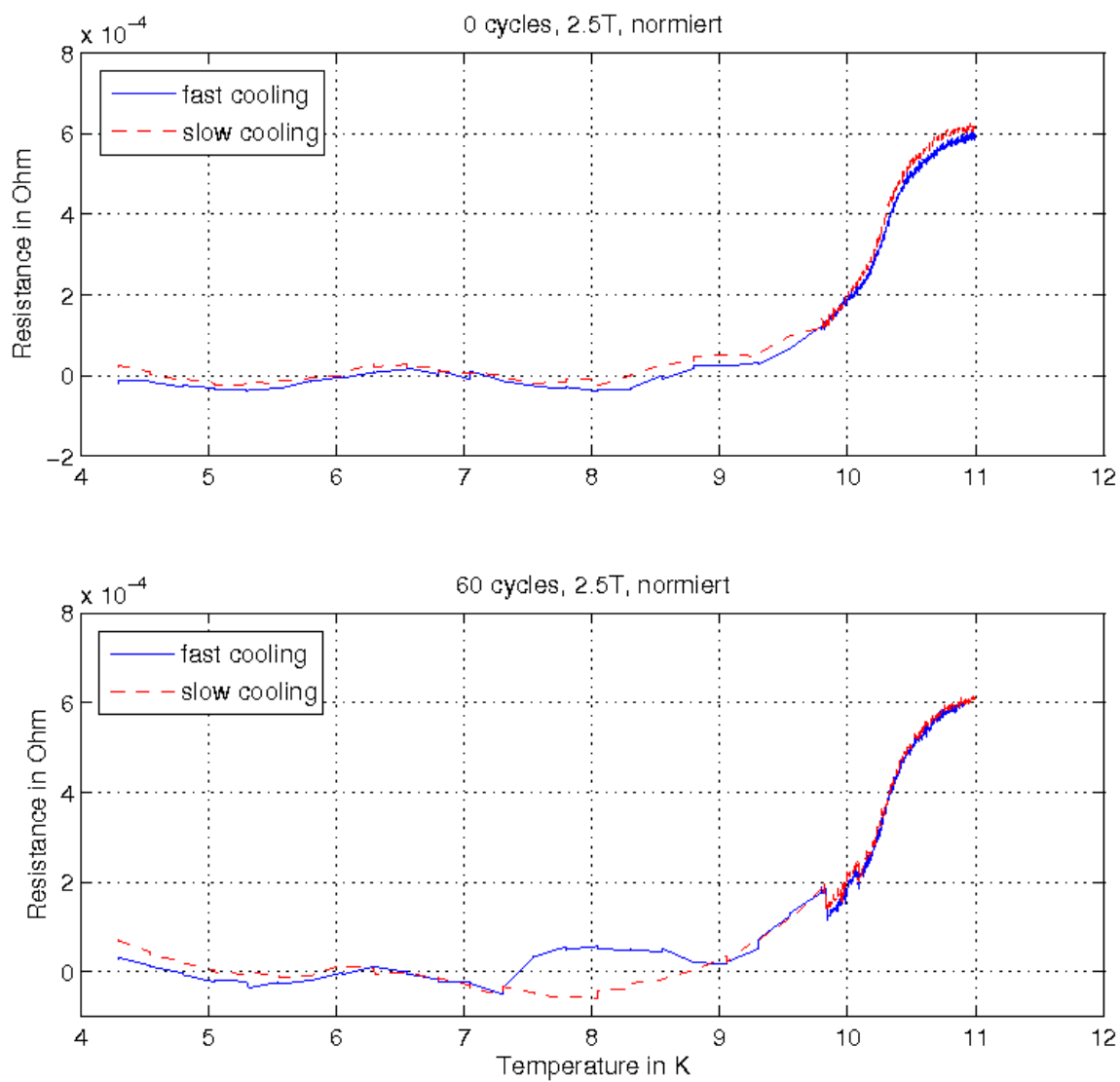


Figure 24: Comparison of runs without and with cycling. The upper figure shows that the velocity of cooling did not make a difference.

List of Figures

1	Shubnikov-Phase (“mixed state”) in a Type II superconductor with the Abrikosov lattice.	3
2	Phase diagrams of a conventional low temperature and a high T_c type-II superconductor.	4
3	Visualization of the transverse and longitudinal vortex shaking. In both geometries the vortices drift towards the center of the strip. Shown is one vortex at subsequent times $t\omega/\pi = 0, 1, 2, \dots$. Top: If h_{ac} is transverse to J , the vortices “walk” in the xz plane (the vortices are straight since here $J_c \ll h_{ac}$, H_a is assumed). Bottom: If h_{ac} is parallel to J , the vortices periodically tilt in the yz plane and at the same time move along x . From [15].	8
4	Scheme of the vortex shift in a slab when the longitudinal ac magnetic field is increased from h_{ac} to $h_{ac} + \delta h$. Shown is the projection on the xy plane of a vortex (bold solid line) which tilts more away from the z axis and at the same time shifts from $x = x_0$ to $x = x_0 + \delta x_0$. The projected shifts of some vortex line elements are shown as dashed arrows with components δx_0 and $\delta y(z)$, $\delta y(z) = -\delta y(-z)$. These arrows are along the Lorentz force, which is perpendicular to the local current density $j_c(z)$ (solid arrows) lying in the xy planes at the angle $\phi(z)$ to the y axis. From [15].	9
5	Structure of YBCO with the CuO_2 planes. In NdBCO the Yttrium atoms are replaced by Neodymium.	10
6	Location of the melting transition in the magnetic phase diagram. (Data from specific-heat measurements.)	10
7	Sketch of the experimental setup, side view.	11
8	Example of the first unsuccessful measurements at 0 Tesla, where the resistance becomes “negative”. T_c is at 96K.	13
9	Scattered data in the graph of the 9T (2/1000/0.1) measurement.	15
10	Results for the measurements of the resistance of NdBCO without shaking. Background and offset distracted.	16
11	Results for the measurements at 7T with and without shaking. Upper right: Zoom into the region of the melting transition. Crosses representing the run without shaking, stars the run with shaking. Bottom: Difference between the normal and the resistance with shaking.	17

12	This figure shows the difference between measurements with and without shaking for 9T main field. Obviously, the shaking did not have an observable effect.	18
13	The crystal structure of $LuNi_2B_2C$. Filled circles are Ni atoms, the largest open circles are Lu atoms. The Ni-B-C framework is indicated by the bonds between the atoms. [26] .	20
14	Temperature vs Resistance of the LuNiBC crystal from 0 to 7T, with shaking.	21
15	Temperature vs Resistance of the LuNiBC crystal at 2T, with shaking. \times represent pre-shaking results, $+$ results after shaking. The dotted line follows the \times as an aid.	22
16	To approach of the current density J_c towards J_c^{st} is schematically shown as a function of field B for a fixed J_c^{st} . (i) At point A, $J_c > J_c^{st}$ and J_c decreases when the field is increased (path b) or decreased (path a). Similarly, at point C, $J_c < J_c^{st}$ and J_c increases when the field is increased (path d) or decreased (path c). (ii) The same is shown under the application of an oscillatory field. [27]	23
17	Results for the two slow cooling measurements, the feature can be seen at $\approx 9.8K$	24
18	Results of the second LuNiBC experiments. Adjusted data for all four runs.	25
19	Zoom into the area around the feature. Within the experimental scatter, the two features (after fast and slow cooling) are nearly identical.	26
20	In-plane resistance $\rho(H, T)$ of a clean high-temperature superconductor. After [28].	29
21	In-plane resistance $\rho(H, T)$ of a high-temperature superconductor with pinning centers, without shaking.	29
22	Sketch of the experimental setup, top view.	30
23	Comparison of fast and slow cooling in the second $LuNi_2B_2C$ experiment. The feature at 9.8K is both times clearly visible. .	31
24	Comparison of runs without and with cycling. The upper figure shows that the velocity of cooling did not make a difference.	32

References

- [1] J. Bardeen, L. N. Cooper and J. R. Schrieffer: Phys. Rev. **106**, 162 (1957); **108**, 1175 (1957)
- [2] N. W. Ashcroft: Phys. Rev. Lett. **21**, 1748 - 1749 (1968)
- [3] Quantum Design: PPMS Hardware & Options Manuals, 2000
- [4] Werner Buckel: Supraleitung, 5. Edition, VCH, 1993
- [5] Stefan Menzi: Messung der Richtungsabhängigkeit der spezifischen Wärme von $\text{YBa}_2\text{Cu}_3\text{O}_7$: Ein Indikator für s- oder d-Wellen Supraleitung?, Bachelorarbeit Uni Zürich, 2005
- [6] J. G. Bednorz and K. A. Müller: "Possible high T_c superconductivity in the BaLaCuO system". Z. Physik, B **64**: 189-193.(1986)
- [7] A. Abrikosov: On the magnetic properties of superconductors of second group. Sov. Phys. JETP **5**, 1174-1182, (1957).
- [8] J. Figueras *et al.*: Nature **2** 402 (2006) www.nature.com/naturephysics doi:10.1038/nphys311
- [9] F. Lindemann: Z.Phys, 11, 609, (1910)
- [10] <http://phycomp.technion.ac.il/phsorkin/thesis/node4.html>
- [11] Hugo Keller: Magnetische Flusslinien in Hochtemperatur Supraleitern, Vierteljahrsschrift der Naturforschenden Gesellschaft in Zürich, 153-160 (4) (2000)
- [12] A. T. Fiory and B. Serin: Phys. Lett.**25A**, 557 (1967)
- [13] M. Willemin, C. Rossel, J. Hofer, H. Keller, A. Erb, and E. Walker: Phys. Rev. B **58**, R5940 (1998)
- [14] Brandt, P. Esquinazi and H. Neckel: J. Low Temp. Phys. **63**, 187 (1986)
- [15] G. P. Mikitik and E. H. Brandt: J. Low Temp. Phys. **139**, 221 (2005)
- [16] E. H. Brandt and G. P. Mikitik: Phys. Rev. Lett. **89** 027002-1 (2002)
- [17] Andrei Mourachkine: Room-Temperature Superconductivity, Cambridge International Science Publishing (2004)

- [18] K. Yamafuji, N. Sakamoto, and T. Kawashima: Phys. Lett. **36A**, 341 (1971)
- [19] C.P. Bean: Phys. Rev. Lett. **8**, 250 (1962); Rev. Mod. Phys. **36**, 31 (1964).
- [20] A. Schilling *et al.*: Nature **382** 791 (1996)
- [21] U. Welp *et al.*: Phys. Rev. Lett. **76** 4809 (1995)
- [22] G. W. Crabtree *et al.*: Journal of Low Temperature Physics (1996)
- [23] M. Willemin *et al.*: Phys. Rev. Lett. **81**, 4236 (1998)
- [24] S. Samarappuli, A. Schilling and H. R. Ott: Physica C, Volume 201, Issue 1-2, p. 159-165. (1992)
- [25] G. P. Mikitik and E. H. Brandt: Journal of Low Temperature Physics, **139** (2005)
- [26] T. Siegrist *et al.*: Nature **367**, 254-256 Letter (1994)
- [27] G. Ravikumari *et al.*: Phys. Rev. B **63**, 024505 (2000)
- [28] A. K. Pradhan, S. Shibata, K. Nakao and N. Koshizuka: Europhys. Lett, **46** (6), 787-793 (1999)